Journal of Zhejiang University-SCIENCE A (Applied Physics & Engineering)
ISSN 1673-565X (Print); ISSN 1862-1775 (Online)
www.jzus.zju.edu.cn; www.springerlink.com
E-mail: jzus@zju.edu.cn

Characterization of the mean velocity of a circular jet in a bounded basin*

Jun-ning LI†, Jian-min ZHANG†‡, Yong PENG

(*State Key Laboratory of Hydraulics and Mountain River Engineering, Sichuan University, Chengdu 610065, China*)

†E-mail: lijunning626@163.com; zhangjianmin@scu.edu.cn

Received Dec. 5, 2016; Revision accepted Mar. 31, 2017; Crosschecked Sept. 7, 2017

Abstract: A circular jet has broad and important applications in practical engineering. Most research in this area has focused on a free jet, a wall jet or a vertical jet in a bounded domain. In this study, the mean velocities of circular offset jets were studied for four jet exit Froude numbers (*Fr*), three offset heights (*S*) (*S*/*d*=1, 2, 3) and three submergence ratios (*ht*/*S*) (surface jet, mixed jet, and submerged jet) in a bounded basin. Based on the results, we propose a velocity decay formula for a circular jet. The lateral velocity spread was more consistent with Gaussian and Cauchy–Lorentz distributions than the vertical velocity. Moreover, *Fr* had little effect on the decay of the mean velocity for a circular jet when $Re>1\times10^4$. The lateral and vertical spreads showed a quadratic relationship with the streamwise distance for different values of *Fr* at *X*/*d*<10. The positions of maximum mean velocity decay were independent of *Fr* and *S*/*d* when *X*/*d*<10. The spread rate was more uniform in the lateral direction than that in the vertical direction in a certain region for different *S*/*d* and *ht*/*S*. Therefore, the decay, spread, and maximum velocity position of the mean velocity for a circular offset jet can remain stable under different values of *Fr*, offset height, and submergence ratio.

Key words: Circular jet; Velocity decay; Froude number (*Fr*); Offset height; Submergence ratio
http://dx.doi.org/10.1631/jzus.A1600761 **CLC number:** TV131.3

1 Introduction

Jets can be classified into free, wall, and offset jets. A free jet is formed when the exit of the discharge jet is sufficiently far away from a boundary. A wall jet is formed when the exit is close to a boundary, and an offset jet is formed when a jet discharges into an ambient medium above the surface of a boundary. An offset jet has characteristic features that are similar to those of free jets close to the nozzle exit, and similar to those of wall jets beyond the reattachment point. Therefore, an offset jet has the characteristics of both free and wall jets and is more complex than free or wall jets alone.

Because offset jets can be used in many fields, many studies of their flow and concentration fields have been carried out in the context of practical engineering applications. For example, Zare and Baddour (2007) argued that a 3D submerged jet is similar to a central jet, and analyzed vortex characteristics in the vertical and horizontal directions. Nyantekyi-Kwakye *et al.* (2015) studied the backflow region of the 3D turbulent flow characteristics of an offset rectangular jet exit. They found that the decay rate of the maximum streamwise mean velocity increased with the offset height ratio, but was different from the spread of the velocity in the lateral and vertical directions. Agelin-Chaab and Tachie (2011a) investigated circular jet characteristics with different offset heights and Froude number (*Fr*) values. Their results showed that the *Fr* number was independent of the local streamwise maximum mean velocity (U_m) decay, especially when *X*/*d*<60, where *X* is the streamwise

‡ Corresponding author
* Project supported by the National Natural Science Foundation of China (No. 51579165)
ORCID: Jun-ning LI, http://orcid.org/0000-0003-2845-5691; Jian-min ZHANG, http://orcid.org/0000-0002-9154-231X

direction and d is the circular jet diameter. The decay rate in the vertical direction was consistent with stable wall jets and larger than that reported by Davis and Winarto (1980). The decay rate in the lateral direction was in agreement with that obtained by Davis and Winarto (1980). Raiford and Khan (2009) performed nine experiments under different Reynolds numbers (*Re*) and submergence ratios, and determined the velocity profiles and growth rates of velocity profiles in the horizontal and vertical planes. Camino *et al.* (2012) noted that the amount of energy dissipated could be determined by jet diffusion in a confined chamber with different expansion ratios and entry locations. They obtained detailed velocity measurements for an eccentric jet to assess the evolution of velocity and turbulence characteristics for a central symmetrical jet. Law and Herlina (2002) observed the characteristics of a circular 3D turbulent wall jet using a combined particle image velocimetry (PIV) and planar laser induced fluorescence (PLIF) approach to measure the velocity and concentration fields simultaneously. They showed that both the velocity and concentration profiles were similar in the streamwise and lateral directions when the distance was several times the diameter of the jet exit. Tachie *et al.* (2004) reported the effects of surface roughness on the mean flow characteristics of a turbulent plane wall jet created in an open channel. Their results showed that surface roughness increased the skin friction coefficient and the inner layer thickness, but the jet half-width was nearly independent of surface roughness. Katakam and Rama (1998) carried out theoretical and experimental research on a hydraulic jump in suddenly enlarged stilling basins and determined that the flow energy dissipation rate and the downstream flow pattern were relatively stable. Mi and Zheng (1989; 1990) reported an experimental study of a rectangular nozzle jet with different aspect ratios. They found that the turbulence intensity increased with increasing aspect ratio when the ratio was less than 8, but decreased slightly when the ratio exceeded 8. A numerical comparison between the mean flow characteristics of offset jets issuing from circular and square-shaped nozzles of equal area and mean exit velocity revealed that the spread rate, flow entrainment, and mixing rate of an offset jet issuing from a circular nozzle were lower than those from a square-shaped nozzle (Mohammadaliha *et al.*, 2016). Hager (1985), Ohtsu *et al.* (1999), and Ferreri and Nasello (2002) studied a spatial hydraulic jump in a stilling basin with sudden expansion and an abrupt drop. Their research revealed that the near-floor velocity decreased gradually with an increase in the height of the drop-sill in the stilling basin. A new energy dissipator was proposed, named the multi-horizontal submerged jet (Chen *et al.*, 2010a; 2010b). The mean flow characteristics of a turbulent dual jet consisting of a plane wall jet and a parallel offset jet were studied by Kumar (2015). Huai and Li (2001) and Guo (2014) carried out numerical simulations to investigate vertical jets.

Previous studies have focused on either an unbounded jet, a wall jet, or a vertical jet in a bounded domain. However, studies of a horizontal circular jet with an offset have been relatively scarce. In this paper, the mean velocities of a horizontal circular jet with an offset height (S/d=1, 2, 3, where S is the offset height) in a bounded basin (B/d=4.8, where B is the width of the bounded basin) were measured for different Fr values and submergence ratios (h_t/S, where h_t is the tailwater depth). The mean velocities in the mainstream, lateral, and vertical directions were measured and compared with those obtained in previous research on rectangular jets. The behavior of the mean velocity distribution was also analyzed for different values of Fr, S/d, and h_t/S.

2 Experimental configuration

A sketch of the experimental setup using the Cartesian coordinate system is shown in Fig. 1, where U_j is the mean velocity at the jet exit. The experimental apparatus comprised an upstream reservoir, a jet section, a stilling basin, a tailwater section, and a flow test section. The jet section was a circular tube with a length of 1.3 m and diameter of 0.1 m. The flow test section was a bounded basin 3.5 m long, 0.48 m wide, and 0.7 m deep, constructed from transparent acrylic sheets to enable clear observation of the flow. The origin of the coordinate system (X, Y, and Z are streamwise, lateral, and vertical directions, respectively) was selected at the centerline of the jet exit. The measurement points for velocities were in

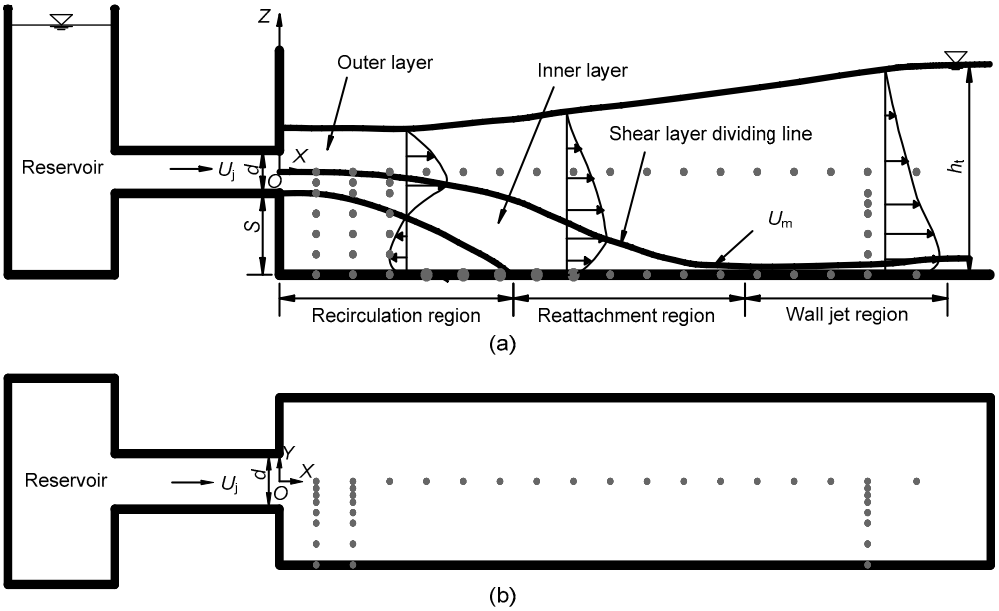

Fig. 1 Sketch of the experimental circular jet with offset
(a) Side view; (b) Plan view. Gray dots denote the measuring points for X<1.6 m

the two planes of Y=0 and Z=0 at X=0–2.4 m, where, when X=0–1.6 m, the interval was 0.1 m, and when X=1.6–2.4 m, the interval was 0.2 m. The measurement points were at Z=0, −0.015, −0.035, −0.05, −0.075, and −0.1 m. When Z<−0.1 m, the interval was 0.05 m in the plane of Y=0. The measurement points were at Y=0 and Y=0.02–0.06 m at an interval of 0.01 m; when Y>0.06 m, the other points were at Y=0.09, 0.12, 0.18, and 0.24 m in the plane of Z=0. In other words, there were 10 measurement points in the plane of Z=0, and 7 (S/d=1), 9 (S/d=2), and 11 (S/d=3) in the plane of Y=0 along the flow direction of each section.

The water depths were measured using a steel ruler with an accuracy of 1 mm. The velocity was measured using an LGY-II velocity instrument (a propeller flow meter) constructed at the Nanjing Hydraulic Research Institute, China. The propeller radius was 12 mm. The accuracy of the measured velocity was 0.01 m/s with a measurement time of 5 s, and the range of measurement velocity was 0–7 m/s. During the experiments, three ratios of offset height to jet exit diameter (S/d=1, 2, and 3), three submergence ratios of tailwater depth to offset height (h_t/S), and four values of Fr (Fr=$U_0/(gd)^{0.5}$, where U_0 is the mean cross-sectional velocity, and g is the acceleration of gravity (g=9.81 m/s^2); Fr=2.57, 3.46, 4.06, and 5.30) were tested. As the tailwater depth increased, the flow pattern in the stilling basin evolved from that of a surface jet to a mixed jet and then to a submerged jet. The propagation of the jet was affected by the tailwater and the sidewalls of the stilling basin; thus, the jet in this experiment can be considered an offset jet in a bounded basin. Detailed test parameters are shown in Table 1.

Table 1 Test parameters

Test	S/d	h_t/S			Fr
		Surface jet	Mixed jet	Submerged jet	
1–3	1	2.60	2.80	3.30	2.57
4–6	2	1.90	2.15	2.38	2.57
7–9	3	1.62	1.78	1.95	2.57
10–12	1	3.00	3.60	4.05	3.46
13–15	2	1.98	2.20	2.45	3.46
16–18	3	1.67	1.83	1.97	3.46
19–21	1	3.00	3.55	4.00	4.06
22–24	2	2.00	2.30	2.50	4.06
25–27	3	1.72	1.88	2.02	4.06
28–30	1	3.30	3.90	4.10	5.30
31–33	2	2.05	2.30	2.55	5.30
33–36	3	1.83	1.93	2.10	5.30

3 Results and discussion

The Fr value, S/d, and h_t/S of the circular jet were varied in the experiments (Table 1). The flow pattern in the basin and the distribution of the mean velocity in the three directions (X, Y, and Z) will be discussed. In addition, the influence of the geometric and hydraulic parameters on the mean velocity of the jet will be discussed and compared to the results of previous research on rectangular jets.

3.1 Initial conditions

Because the shape of the jet exit has a significant influence on the flow characteristics, it is necessary to verify the velocity distribution of the jet exit with the 1/7th power law for pipe velocity distribution. In the diameter range of the jet exit, the plane radial mean velocity was nondimensionalized using the maximum velocity of the cross section. In this experiment, Re was 2.5×10^5–5.0×10^5. Thus, the jet exhibited fully developed turbulent pipe flow.

With Fr=4.06 and S/d=2, the velocity distribution at X/d=0.5 was compared with the results obtained by Agelin-Chaab and Tachie (2011a), and the velocity of the jet section was compared with the 1/7th power law (Fig. 2). The velocity at the exit jet could not be measured due to the limited measurement space, so the initial test section was located at X/d=0.5.

Fig. 2 shows that the error between the average velocity calculated by the pipe flow calculation formula and the theoretical value was 0.9%. The average velocity of the jet exit can be obtained from the pipe flow calculation formula:

$$V=\frac{\int_0^{r_0}U_x 2\pi r\mathrm{d}r}{A}, \tag{1}$$

where V is the average velocity of jet exit, U_x is the local streamwise mean velocity, r is the radical length, $r_0=d/2$, and A is the area of the circular jet exit.

The experimental value of U_j/U_0 obtained for Fr=4.06 and S/d=2 was 1.17, which is consistent with the value of 1.22 obtained by the 1/7th power law approximation for fully developed turbulent pipe flow. Therefore, the measuring instrument and method for this experiment are reasonable and acceptable.

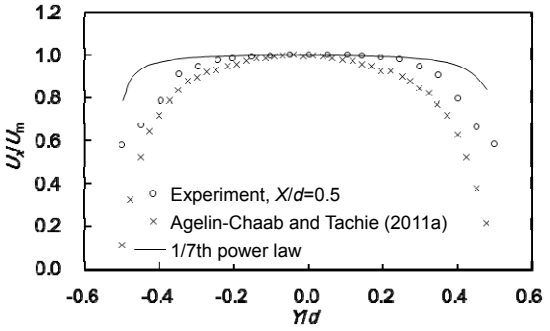

Fig. 2 Profiles of streamwise velocity at X/d=0.5

3.2 Mean velocity

3.2.1 Streamwise velocity decay

The decay law of the maximum mean velocity U_m for the main flow in the basin was of primary interest in this study. The streamwise profile of U_m is shown in Fig. 3. The relationship between U_m/U_j and X/d for a circular jet is as follows (where erf is the error function or Gauss error function):

$$\frac{U_m}{U_j}=\left[1+\mathrm{erf}\left(\left(12-\frac{X}{d}\right)\Big/4\right)\right]\Big/2, \tag{2}$$

$$\frac{U_m}{U_j}=0.405\left(\frac{X}{d}\right)^{1/5}\left[1+\mathrm{erf}\left(\left(12-\frac{X}{d}\right)\Big/4\right)\right]. \tag{3}$$

When $0<X/d<24$, the fitted curve is described by Eq. (2). The error fitting is not satisfactory. When $0<X/d<10$, the fitted curve is described by Eq. (3), optimized by Eq. (2). The error fitting is within 10%.

3.2.2 Velocity distribution in lateral and vertical directions

The location of the maximum flow velocity U_m and its decay are important aspects of the mainstream flow velocity. The normal distribution model of a Gaussian distribution for a free jet can be used as follows:

$$\frac{U_x}{U_m}=\exp\left(-\frac{Z}{Z_{1/2}}\right)^2, \tag{4}$$

where $Z_{1/2}$ is the vertical half-width.

Law and Herlina (2002) indicated that the velocity distribution for a wall jet was independent of Re

in the mainstream direction. They showed that the velocity profiles in the lateral and vertical directions are suitable for Cauchy–Lorentz distribution:

$$\frac{U_x}{U_\mathrm{m}}=\frac{1}{1+\left(0.965\frac{Z}{Z_{1/2}}\right)^2}. \tag{5}$$

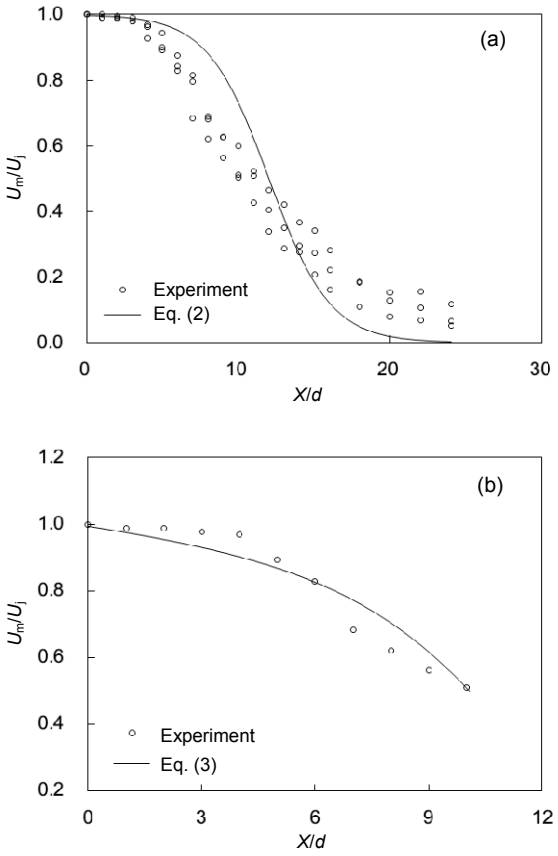

Fig. 3 Profile of maximum mean velocity
(a) Eq. (2); (b) Eq. (3)

The velocity distributions in the lateral (U_x/U_m–$Y/Y_{1/2}$, where $Y_{1/2}$ is the lateral half-width) and the vertical (U_x/U_m–$Z/Z_{1/2}$) directions for a circular jet with Fr=4.06 and S/d=2 are shown in Fig. 4. The distribution of dimensionless U_x/U_m is between the Gaussian distribution and Cauchy–Lorentz's function (Cauchy-L). In addition, the decay of the lateral velocity (U_x/U_m=1) is at $Y/Y_{1/2}$<0.5 when X/d<5, but the decay of the vertical velocity (U_x/U_m) at $Z/Z_{1/2}$<−0.4 agreed well with the Gaussian distribution and Cauchy–Lorentz's function. The horizontal velocity profiles have a slight tendency to be smaller than a Gaussian distribution for free jet velocity profiles near the centerline, and larger away from the center line when $Y/Y_{1/2}$<0.5, as found by Raiford and Khan (2009) when X/d=24.

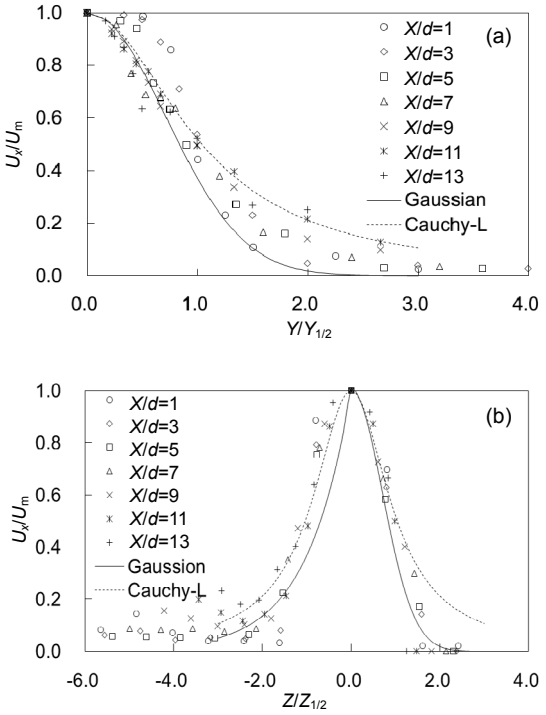

Fig. 4 Velocity distributions in the lateral (a) and the vertical (b) directions

The basin wall had no obvious effect on the lateral velocity spread, although there was an effect on the vertical direction to the bottom of the basin. This was mainly because the cross velocity direction of a circular jet is uniform and the surrounding conditions have little inhibitive effect on the velocity spread. After a certain distance (X/d>8), the vertical velocity profiles did not agree well with the Gaussian or Cauchy–Lorentz distribution. The flow turbulence was severe in the basin because of the stress caused by the jet and the surrounding flow, the gravity of the jet, and the mutual mixing between the flow in the basin and the backflow. Beyond the point where jets begin to interact with boundaries, the profiles no longer behave as a Gaussian distribution for a free jet in the vertical direction (Raiford and Khan, 2009). Therefore, the velocity spread of the circular offset jet in the

vertical direction was different from that of the free jet and the wall jet.

3.3 Influencing factors

Based on experiments, the main factors influencing the maximum flow velocity decay in the streamwise direction of circular and rectangular jets are *Fr*, offset height *S*, and the degree of submergence h_t/S.

3.3.1 Dependence on the approach Froude number *Fr*

The position and distribution of U_m for the circular and rectangular jets are shown in Fig. 5, when Re=2.5×10^5–5×10^5 (in this study, C stands for the circular jet, and R for the rectangular jet). The effect of *Fr* on the decay law for the maximum velocity of the circular jet (*S*/*d*=2, mixed jet) was small. This conclusion is consistent with the results obtained by Mi and Zheng (1990) when Re=1.5×10^4–6.5×10^4. The flow characteristics were observed to be nearly independent of the Reynolds number (Agelin-Chaab and Tachie, 2011b) when Re=1×10^4 and 2×10^4, but not when Re=0.5×10^4. Regardless of the type of jet exit, the dispersion of U_m decay for the circular and the rectangular jets was less than 5% in the mainstream direction. For different *Fr*, the decay law of U_m in the mainstream direction was almost the same. When the flow pattern evolved from that of a surface jet to a mixed jet, and then to a submerged jet with *S*/*d*=2, the distribution of U_m was also independent of *Fr* when Re>1×10^4 (Fig. 5c). Thus, in the case of identical geometric parameters such as jet shape and offset height, the lateral and vertical velocity distributions were independent of *Fr* when Re>1×10^4. This can be partly explained by the more uniform velocity distribution and higher jet momentum flux at a higher Reynolds number.

The position of the maximum mean velocities Z_m remained at the centerline of the jet exit when *X*/*d*<10 and was independent of *Fr*, but changed when 10< *X*/*d*<15 (Figs. 5b and 5d). Due to the strong turbulence intensity during the operation of the circular jet, the fluctuations in the position of maximum velocity increased as *Fr* increased. For the rectangular jet, the position of maximum velocity gradually shifted from the jet exit to the basin bottom. For example, with the same value of *S*/*d*=2, the vertical distance from the bottom to the position of U_m for a circular jet was

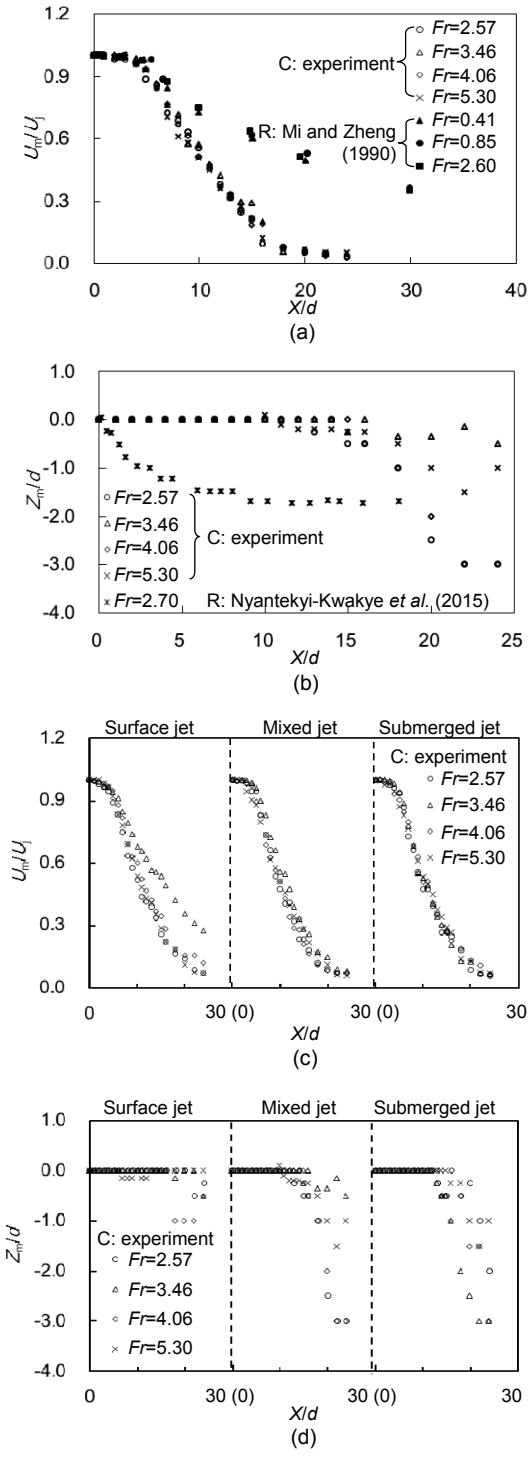

Fig. 5 Distribution (a) & (c) and position (b) & (d) of maximum mean velocity for a circular jet and a rectangular jet with different *Fr* values: (a) circular jet (*S*/*d*=2, mixed jet, *Fr*=2.57–5.30) and rectangular jet (b/b_0=0.5, *Fr*=0.41–2.60); (b) circular jet (*S*/*d*=3, mixed jet, *Fr*=2.57–5.30) and rectangular jet (b/b_0=6, *Fr*=2.70); (c) & (d) circular jet (*S*/*d*=3) (*b* is the width for rectangular jet, and b_0 is the height for rectangular jet)

much larger than that for a rectangular jet as *Fr* changed. The mainstream of the rectangular jet was not stable and descended sharply after the jet exit. However, the mainstream of the circular jet remained unchanged and continued for a certain distance at a constant height.

The effect of *Fr* on the velocity spread in the lateral and vertical directions is shown in Fig. 6. For *Fr*=2.57–5.30, the spread in the lateral direction changed slightly (Figs. 6a and 6c), and the spread rate increased monotonically with *X*/*d* (Figs. 6b and 6d). This phenomenon was caused mainly by the strong mixing of the mainstream flow and the surrounding water at the end of the basin.

When the flow condition was a mixed jet with *X*/*d*=2 and *X*/*d*<10, the fitting curves of the lateral and the vertical spreads could be expressed as follows:

$$\frac{Y_{1/2}}{d}=0.0042\left(\frac{X}{d}\right)^2-0.0132\frac{X}{d}+0.472, \quad (6)$$

$$\frac{Z_{1/2}}{d}=-0.0047\left(\frac{X}{d}\right)^2+0.0161\frac{X}{d}-0.479. \quad (7)$$

Therefore, the lateral and vertical spreads showed a quadratic relationship with the streamwise distance for a circular jet with an offset height. However, for the rectangular jet, beyond the region X/b_0>5, the jet spread linearly with the streamwise distance for the h/b_0=2 (*h* is offset height for rectangular jet) offset jet (Nyantekyi-Kwakye *et al.*, 2015).

3.3.2 Offset height

The velocity distribution and position of U_m for different offset heights (*S*/*d*=1, 2, and 3) are shown in Fig. 7. For different *S*/*d*, the decay rates of U_m in the streamwise direction for a circular jet and a rectangular jet (Nyantekyi-Kwakye *et al.*, 2015) are shown in Fig. 7a.

The decay rate of the maximum velocity increased with increasing offset height, but not obviously for the circular jet. The dispersion of U_m/U_j for the circular jet was 5%. The same conclusion can be drawn from Fig. 7c, where the flow pattern is of a mixed-jet type with *Fr*=2.57, 4.06, and 5.30. However, the dispersion of U_m/U_j for a rectangular jet (Nyantekyi-Kwakye *et al.*, 2015) becomes large from *X*/*d*=5 to *X*/*d*=30. Near the jet exit, the decay rate of the streamwise velocity for the circular jet was clearly smaller than the streamwise velocity for the rectangular jet when *X*/*d*<8. When the offset height was low

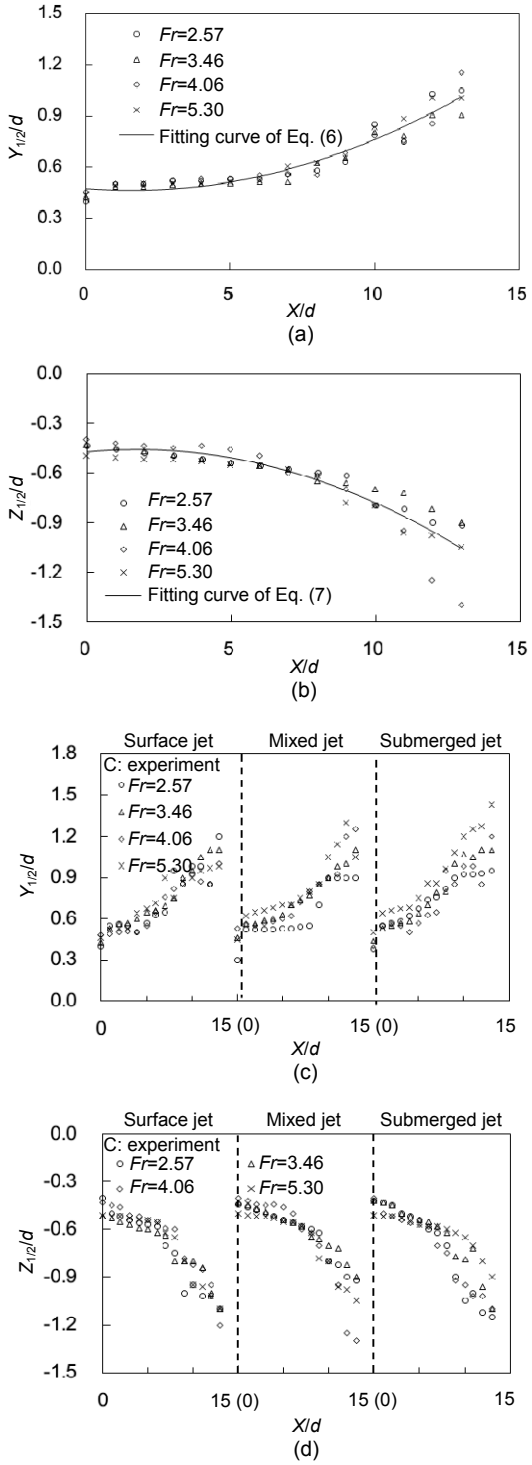

Fig. 6 Effect of *Fr* on the spread in the lateral (a) & (c) and vertical (b) & (d) directions: (a) & (b) circular jet (*S*/*d*=2, mixed jet); (c) & (d) circular jet (*S*/*d*=3)

(h/b_0=2), the jet core moved down quickly, but not when the offset height increased to h/b_0=4. The decay rate of the streamwise velocity with the circular jet was larger than that of the streamwise velocity with the rectangular jet when X/d>10. The main reason is that the cross-sectional velocity distribution in a circular jet is more uniform than the cross-sectional velocity distribution in a rectangular jet. The suppression effect of the surrounding flow on the jet flow is small when the jet is circular. After a certain distance, the inertia of a circular jet becomes weak and the circular jet flow mixes with the surrounding flow. However, a rectangular jet exit appears as a "duck mouth" that is unstable in the gravity direction. When the offset height is smaller, the lift of the surrounding flow is weaker, and the flow core moves quickly to the bottom of the basin. When the offset height increases, a cushion effect is caused by the surrounding flow, and the surrounding flow can avoid contacting the bottom of the basin directly. Clearly, the offset height S/d had little effect on the decay rate of the maximum velocity for the circular jet, but a large effect on that for the rectangular jet.

The effects of different values of S/d on the position of maximum velocity for a rectangular jet (Nyantekyi-Kwakye *et al.*, 2015) and a circular jet are shown in Fig. 7b. For a circular jet with S/d =1, 2, and 3, the position of maximum velocity remained near the centerline of the exit jet when X/d<10, but the position changed considerably when X/d>10. This conclusion is consistent with the results obtained by Raiford and Khan (2009) when S/d=2, 3, and 4. This phenomenon is caused mainly by the strong mixing of the mainstream flow and the surrounding water at the end of the basin. A similar result is shown in Fig. 7d, where the flow pattern is of a mixed-jet type with Fr=2.57, 4.06, and 5.30. For a rectangular jet with h/b_0=0, 2, and 4 (Nyantekyi-Kwakye *et al.*, 2015), when X/d<10, the position of maximum velocity gradually shifts to the bottom of the basin under the action of gravity, but the change of position is independent of h/b_0. When X/d>10, the position of maximum velocity rises at h/b_0=2 and descends at h/b_0=4.

The spread of the mean velocity with the rectangular and circular jets for different values of S/d is shown in Fig. 8. The spread rate in the lateral direction was more uniform than that in the vertical direction for a certain region. The current experiments

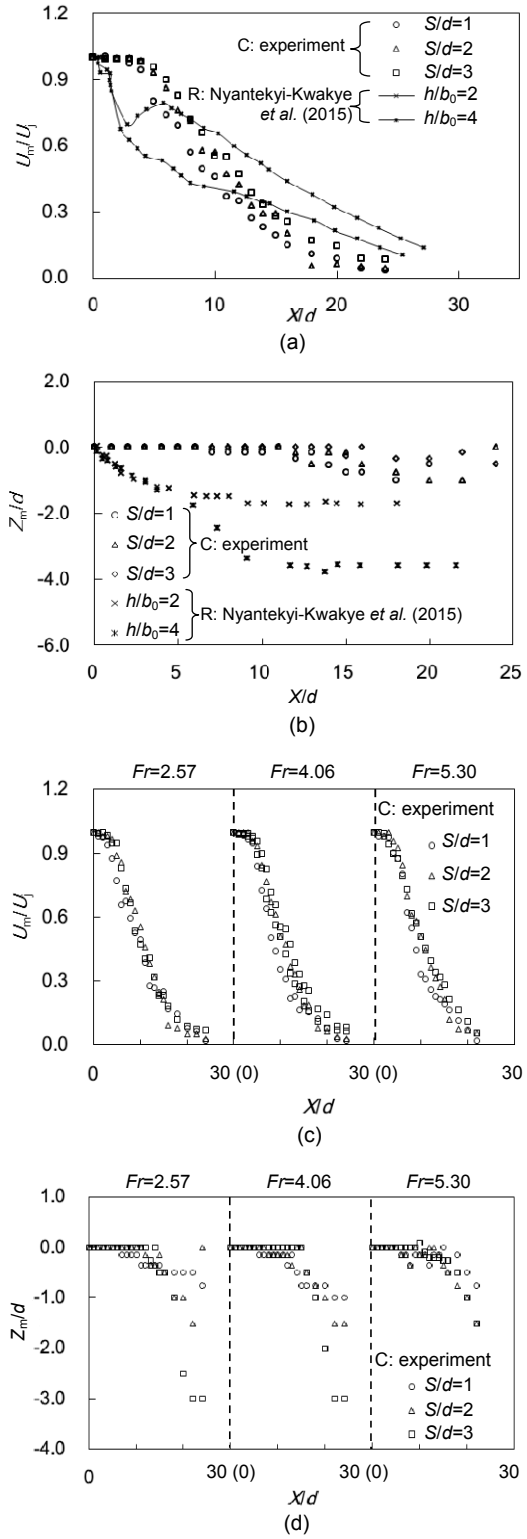

Fig. 7 Distribution (a) & (c) and position (b) & (d) of U_m for circular and rectangular jets with different offset heights S: (a) circular jet (Fr=3.46, mixed jet) and rectangular jet (b/b_0=6); (b) circular jet (Fr=3.46, mixed jet) and rectangular jet (b/b_0=6); (c) & (d) circular jet (mixed jet)

reveal that $Y_{1/2}$ increases with increasing S/d for the circular jet. The relationship between $Y_{1/2}$ and the offset height when S/d=3 is consistent with the values reported by Raiford and Khan (2009) for S/d=1, 2, and 3 when X/d<20. The spread rate in the lateral direction is smaller than that of a rectangular jet with a similar offset height (Nyantekyi-Kwakye *et al.*, 2015).

Figs. 8a and 8c show that S/d had a different effect on the spread rate of the mean velocity for the circular and the rectangular jets. In the lateral direction, for the circular jet, the offset height (S/d=1, 2, and 3) had little effect on the spread rate of the mean velocity. For the rectangular jet, the spread rate was estimated to be 0.116, 0.114, and 0.096 with h/b_0=0, 2, and 4, respectively. Therefore, the spread rate was uniform in a certain region. This observation is partly explained by the spread rate in the lateral direction being minimally affected by the backflow.

Figs. 8b and 8d show the results where the flow pattern was of a mixed-jet type with Fr=2.57, 3.46, 4.06, and 5.30 in the vertical direction, and the directions of deviation of the centerline for the rectangular jet and the circular jet at half-width were opposite. For the circular jet, in the case of S/d=2, the vertical spread was larger than the cases of S/d=1 and 3. The effect of intense backflow suppressed the vertical spread of the jet with S/d=1 and 3. The offset height had little effect on the spread rate in the vertical direction when X/d<8. When X/d>8, the spread rate in the vertical direction increased with streamwise distance, but the rate was independent of S/d. This observation can partly be attributed to the bottom of the basin and the backflow suppressing the spread of the offset jet when X/d>8. For the rectangular jet, the jet spread linearly with the streamwise distance for the h/b_0=2 offset jet (Nyantekyi-Kwakye *et al.*, 2015). This trend is consistent with those reported by Agelin-Chaab and Tachie (2011b). The spread of the h/b_0=2 offset jet was suppressed with streamwise distance because of the occurrence of intense backflow (Nyantekyi-Kwakye *et al.*, 2015).

3.3.3 Submergence ratio

Experiments showed that the tailwater depth h_t had a large effect on the flow pattern. For a submergence ratio (h_t/S) between 1.62 and 4.10, the flow pattern evolved from that of a surface jet to a mixed

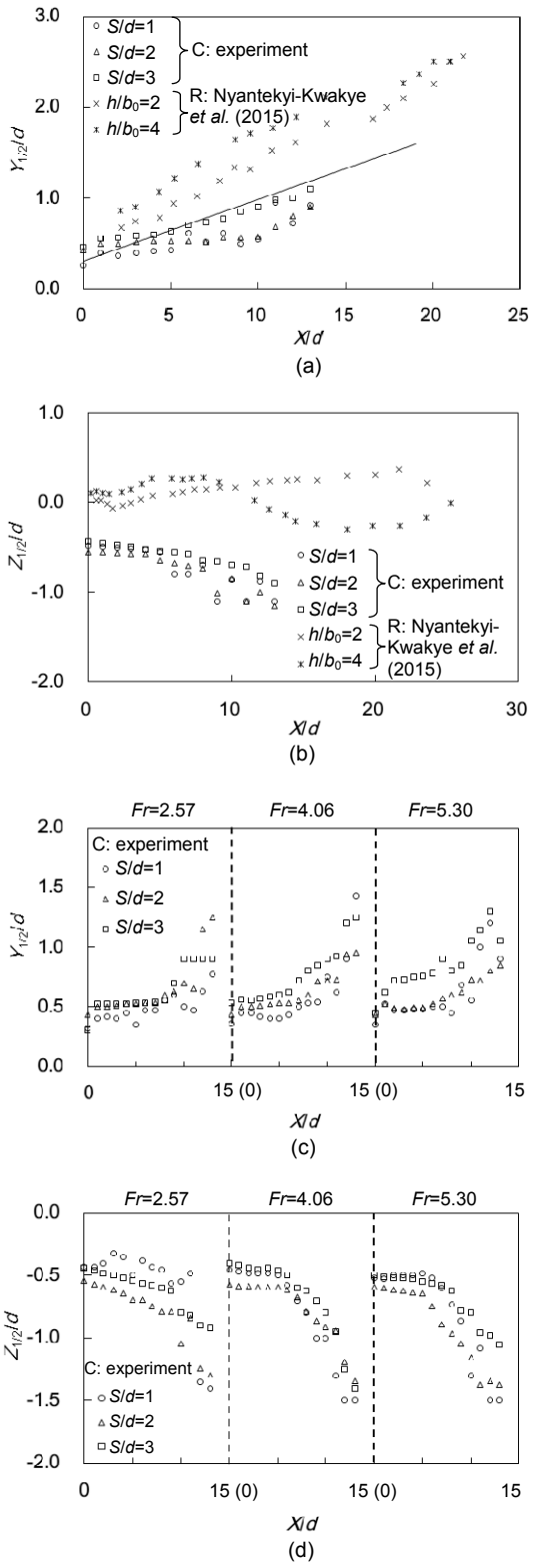

Fig. 8 Effect of the offset height *S* on the spread in the lateral (a) & (c) and vertical (b) & (d) directions: (a) circular jet (*Fr*=3.46, mixed jet); (b) circular jet (*Fr*=3.46, mixed jet); (c) & (d) circular jet (mixed jet)

jet, and then to a submerged jet. The distribution of the dimensionless half-width ($Y_{1/2}/d$, $Z_{1/2}/d$) of the circular jet is shown in Fig. 9. The submergence ratio had little effect on the spread in the lateral direction, but a substantial effect on the spread in the vertical direction. Figs. 9a and 9c show that the submergence ratio (h_t/S) had little effect on the spread of the lateral velocity of the circular jet when Fr=2.57, 3.46, 4.06, and 5.30 at X/d<10. The distribution in the spread of the lateral velocity agrees well with the result of a no baffle sill (h_t/S=0) reported by Agelin-Chaab and Tachie (2011a). The same conclusion can be drawn from Fig. 9c, in which the flow pattern is of a mixed-jet type with Fr=2.57, 3.46, and 5.30 for S/d=2. Therefore, the h_t/S ratio for the circular jet had little effect on the spread in lateral velocity.

For different values of h_t/S, the trends in the vertical velocity for a circular jet were similar to those in the lateral direction when X/d<10. Under the condition of h_t/S=0–4.10 for circular jets, the position of the vertical half-width is shown in Fig. 9b. The dispersion in the vertical velocity caused by h_t/S was about 10% when 0<X/d<10, but reached up to 30% when X/d>10.

The same result is shown in Fig. 9d with Fr=2.57, 3.46, and 5.30 for S/d=2. The difference between Figs. 9b and 9d is that the trend in the variation of vertical velocity is opposite because the values were chosen at the top and bottom, respectively, of the mainstream.

4 Conclusions

In this paper, the velocity distribution of circular offset jets was studied in terms of the decay and spread of the mean velocity in the mainstream, lateral, and vertical directions with four values of Fr, three offset heights S/d, and three submergence ratios h_t/S. The main conclusions are as follows:

1. A formula for the velocity decay of a circular jet was proposed when X/d<10 and when X/d=10–24. The lateral velocity spread was more consistent with the Gaussian and Cauchy–Lorentz distributions than with the vertical velocity.

2. The value of Fr had little effect on the decay of the mean velocity for a circular jet when Re>1×10^4. The position of the maximum mean velocities was

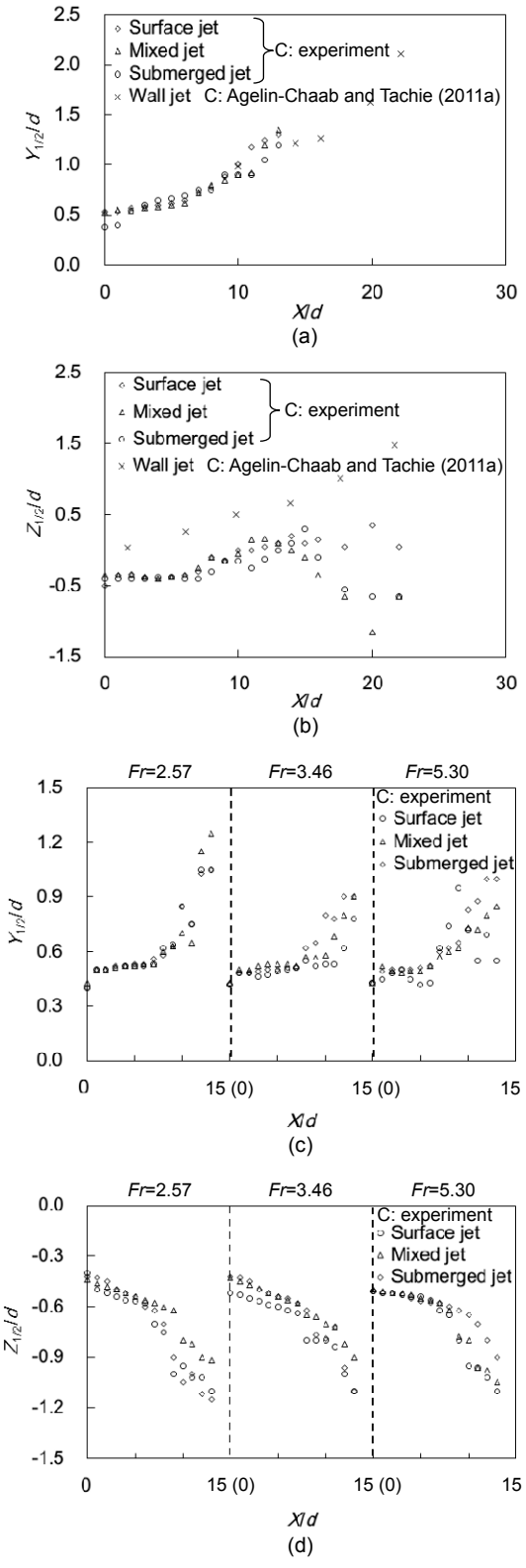

Fig. 9 Influence of submergence ratio (h_t/S) on the spread in the lateral (a) & (c) and vertical (b) & (d) directions: (a) & (b) circular jet (S/d=2); (c) & (d) circular jet (mixed jet, S/d=2)

near the jet centerline when X/d<10 and far from the jet centerline when X/d>10, and was independent of Fr. The lateral and vertical spreads showed a quadratic relationship with the streamwise distance for a circular jet with an offset height.

3. For a circular jet with S/d=1, 2, and 3, the decay rate of the maximum velocity showed no obvious increase with increasing offset height, and the position of maximum velocity remained near the jet centerline when X/d<10, but changed considerably when X/d>10. In addition, the spread rate in the lateral direction was more uniform than that in the vertical direction for a certain region.

4. For different submergence ratios (h_t/S), the spread rate in the lateral direction was more uniform than that in the vertical direction when X/d<10.

Therefore, the decay, spread, and position of the mean velocity for a circular offset jet can remain stable under different Fr, S/d, and h_t/S values.

References

Agelin-Chaab, M., Tachie, M.F., 2011a. Characteristics and structure of turbulent 3D offset jets. *International Journal of Heat and Fluid Flow*, **32**(3):608-620. http://dx.doi.org/10.1016/j.ijheatfluidflow.2011.03.008

Agelin-Chaab, M., Tachie, M.F., 2011b. Characteristics of turbulent three-dimensional offset jets. *Journal of Fluids Engineering*, **133**(5):051203. http://dx.doi.org/10.1115/1.4004071

Camino, G.A., Zhu, D.Z., Rajaratnam, N., 2012. Jet diffusion inside a confined chamber. *Journal of Hydraulic Research*, **50**(1):121-128. http://dx.doi.org/10.1080/00221686.2011.650423

Chen, J.G., Zhang, J.M., Xu, W.L., *et al*., 2010a. Numerical simulation of the energy dissipation characteristics in stilling basin of multi-horizontal submerged jets. *Journal of Hydrodynamics, Ser. B*, **22**(5):732-741. http://dx.doi.org/10.1016/S1001-6058(09)60110-4

Chen, J.G., Zhang, J.M., Xu, W.L., *et al*., 2010b. Scale effects of air-water flows in stilling basin of multi-horizontal submerged jets. *Journal of Hydrodynamics, Ser. B*, **22**(6):788-795. http://dx.doi.org/10.1016/S1001-6058(09)60117-7

Davis, M.R., Winarto, H., 1980. Jet diffusion from a circular nozzle above a solid plane. *Journal of Fluid Mechanics*, **101**(1):201-221. http://dx.doi.org/10.1017/S0022112080001607

Ferreri, G.B., Nasello, C., 2002. Hydraulic jumps at drop and abrupt enlargement in rectangular channel. *Journal of Hydraulic Research*, **40**(4):491-505. http://dx.doi.org/10.1080/00221680209499891

Guo, Y.K., 2014. Numerical simulation of the spreading of aerated and nonaerated turbulent water jet in a tank with finite water depth. *Journal of Hydraulic Engineering*, **140**(8):64-70. https://doi.org/10.1061/(ASCE)HY.1943-7900.0000903

Hager, W.H., 1985. Hydraulic jump in non-prismatic rectangular channels. *Journal of Hydraulic Research*, **23**(1):21-35. http://dx.doi.org/10.1080/00221688509499374

Huai, W.X., Li, W., 2001. Prediction of characteristics for vertical round negative buoyant jets in homogenous ambient. *Journal of Hydrodynamics, Ser. B*, **13**(1):103-110.

Katakam, V., Rama, P., 1998. Spatial B-jump at channel enlargements with abrupt drop. *Journal of Hydraulic Engineering*, **124**(6):643-646. https://doi.org/10.1061/(asce)0733-9429(1998)124:6(643)

Kumar, A., 2015. Mean flow characteristics of a turbulent dual jet consisting of a plane wall jet and a parallel offset jet. *Computers and Fluids*, **114**:48-65. http://dx.doi.org/10.1016/j.compfluid.2015.02.017

Law, A.W.K., Herlina, 2002. An experimental study on turbulent circular wall jets. *Journal of Hydraulic Engineering*, **128**(2):161-174. https://doi.org/10.1061/(asce)0733-9429(2002)128:2(161)

Mi, J.C., Zheng, C.G., 1989. Time-averaged characters in the jets of rectangular pipe nozzles. *Journal of Changsha Normal University of Water Resources and Electric Power*, **4**(6):107-111 (in Chinese).

Mi, J.C., Zheng, C.G., 1990. Factors influencing turbulent rectangular jets. *Aerodynamic Experiment and Measurement & Control*, **4**(3):19-22 (in Chinese).

Mohammadaliha, N., Afshin, H., Farahanieh, B., 2016. Numerical investigation of nozzle geometry effect on turbulent 3-D water offset jet flows. *Journal of Applied Fluid Mechanics*, **9**(4):2083-2095.

Nyantekyi-Kwakye, B., Clark, S.P., Tachie, M.F., *et al*., 2015. Flow characteristics within the recirculation region of three-dimensional turbulent offset jet. *Journal of Hydraulic Research*, **53**(2):230-242. http://dx.doi.org/10.1080/00221686.2014.950612

Ohtsu, I., Yasuda, Y., Ishikawa, M., 1999. Submerges hydraulic jump below abrupt expansion. *Journal of Hydraulic Engineering*, **125**(5):492-499. https://doi.org/10.1061/(asce)0733-9429(1999)125:5(492)

Raiford, J.P., Khan, A.A., 2009. Investigation of circular jets in shallow water. *Journal of Hydraulic Research*, **47**(5):611-618. http://dx.doi.org/10.3826/jhr.2009.3474

Tachie, M.F., Balachander, R., Bergstrom, D.J., 2004. Roughness effects on turbulent plane wall jets in an open channel. *Experiments in Fluids*, **37**(2):281-292. http://dx.doi.org/10.1007/s00348-004-0816-0

Zare, H.K., Baddour, R.E., 2007. Three-dimensional study of spatial submerged hydraulic jump. *Canadian Journal of Civil Engineering*, **34**(9):1140-1148. http://dx.doi.org/10.1139/l07-041

中文概要

题　目： 有限空间内圆形射流时均流速特性研究

目　的： 圆形射流在实际工程中有着重要应用。本文旨在探讨弗劳德数（*Fr*）、跌坎高度和淹没度的变化对有界圆形射流时均流速在主流方向、横向和垂向上的衰减扩散规律的影响，对圆形射流的现有研究成果作进一步的补充。

创新点： 1. 推导出圆形跌坎射流主流方向上流速与射流距离之间的关系；2. 综合考虑了不同 *Fr*、跌坎高度和淹没度对有限空间内的圆形射流流速分布的影响。

方　法： 1. 通过理论推导，验证流速测量方法的可行性和合理性；2. 通过试验的方法，分析 *Fr*、跌坎高度和淹没度的变化对圆形射流时均流速衰减和扩散的影响规律。

结　论： 1. 得出圆形射流主流方向流速衰减的公式；圆形射流的横向流速分布与高斯、柯西-洛伦兹分布吻合较好。2. 当 $Re>1\times10^4$ 时，*Fr* 变化对流速衰减影响较小。3. 当 $X/d<10$ 时，横向和垂向流速扩散与主流方向的距离呈二次方关系。4. 时均流速最大值的位置与 *Fr* 和 *S*/*d* 无关。

关键词： 圆形射流；流速衰减；*Fr*；跌坎高度；淹没度